

## Supporting Information

### The product selectivity zones in Gas Diffusion Electrodes during the electrocatalytic reduction of CO<sub>2</sub>

Tim Möller,<sup>1</sup> Trung Ngo Thanh,<sup>1</sup> Xingli Wang,<sup>1</sup> Wen Ju,<sup>1</sup> Zarko Jovanov<sup>1</sup> and Peter Strasser<sup>1\*</sup>

1. The Electrochemical Energy, Catalysis, and Materials Science Laboratory, Department of Chemistry, Chemical Engineering Division, Technical University Berlin, Berlin, Germany

Corresponding author:

Peter Strasser, [pstrasser@tu-berlin.de](mailto:pstrasser@tu-berlin.de)

#### Contents:

#### 1. Equations for product quantification

**Equation S1.** Production Rate of Gas Products

**Equation S2.** Faradaic Efficiency of Gas Products

**Equation S3.** Faradaic Efficiency of Liquid Products

**Equation S4.** IR-Free RHE potential

#### 2. Experimental Details

2.1 Catalyst synthesis

2.2 Material Characterization

2.3 Electrochemical Characterization

2.4 Product analysis

#### 3. Physical and Chemical Characterization Figures and Tables

*Additional information on the effect of particle catalyst loading*

*Additional information on the effect of ionomer to catalyst ratio*

*Additional discussion on the effect of changes in surface morphology of the catalyst layer.*

*Additional information on the effect of KHCO<sub>3</sub> concentration*

*Additional information on the effect of ionomer to catalyst ratio – ORR*

*Supplementary Tables for the effect of particle catalyst loading and ionomer to catalyst ratio*

# 1. Equations for product quantification

## Equation S1. Production Rate of Gas Products

$$\dot{n}_x = \frac{\dot{V} * C_x}{A * V_M}$$

$\dot{n}_x$ : Generation rate of the product  $x$  / mol  $s^{-1} cm^{-2}$

$\dot{V}$ :  $CO_2$  gas flow rate / L  $s^{-1}$

$C$ : Volume fraction of the product  $x$  detected by GC

$A$ : Geometric area of the electrode /  $cm^2$

$V_M$ : molar Volume / 22.4 L  $mol^{-1}$

## Equation S2. Faradaic Efficiency of Gas Products

$$FE_x = \frac{\dot{n}_x * z_x * F}{j_{total}} * 100\%$$

$FE_x$ : Faradaic Efficiency of the product  $x$  / %

$\dot{n}_x$ : Generation rate of the product  $x$  / mol  $s^{-1} cm^{-2}$

$z_x$ : electrons transferred for reduction to product  $x$

$F$ : Faradaic Constant / C  $mol^{-1}$

$j_{total}$ : Total current density during  $CO_2$  bulk electrolysis / A  $cm^{-2}$

## Equation S3. Faradaic Efficiency of Liquid Products

$$FE_x = \frac{V * \Delta C_x * z_x * F}{\Delta Q} * 100\%$$

$FE_x$ : Faradaic Efficiency of the product  $x$  / %

$V$ : Volume of the electrolyte / L

$\Delta C_x$ : Accumulated concentration of the product  $x$  detected by HPLC or liquid GC / mol  $L^{-1}$

$z_x$ : electrons transferred for reduction to product  $x$

$\Delta Q$ : Total charge transfer during the electrolysis at const. potential or current / C

$F$ : Faradaic Constant / C  $mol^{-1}$

#### **Equation S4. IR-Free RHE potential**

$$E_{RHE} = E_{Ref} + E_{Ag/AgCl} + 0.059 * pH + R * I$$

*E<sub>RHE</sub>*: RHE potential / V

*E<sub>Ref</sub>*: Applied potential against the reference electrode / V

*E<sub>Ag/AgCl</sub>*: Potential of the reference electrode measured against NHE (0.21 V) / V

*pH*: pH-value of the electrolyte

*R*: Ohmic resistance between working and reference electrode /  $\Omega$

*I*: Total Current of the experiment / A

## 2. Experimental Details

### 2.1 Catalyst synthesis.

The catalyst was synthesized according to a previously reported study.<sup>1</sup> In short, an aqueous solution of  $\text{CuCl}_2$  was alkalized by addition of  $\text{NaOH}$ , and reduced to cubic  $\text{Cu}_2\text{O}$  particles with a solution of l-ascorbic acid at room temperature.

### 2.2 Material Characterization

The structure of the electrode surface and cross section were imaged by scanning electron microscopy (SEM). The instrument (JEOL 7401F) was equipped with a COMPO and SEI detector, using an acceleration voltage of 10 kV. The samples were rinsed with milli-Q water and dried in a nitrogen stream to remove any impurities, e.g. remaining  $\text{KHCO}_3$ , prior to SEM analysis. In order to image the cross-section, the gas diffusion electrodes were cut carefully through the catalytic layer of the electrode.

The powder samples were routinely analyzed by powder XRD (D8 Advance Diffractometer, Bruker) to confirm the successful synthesis of the  $\text{Cu}_2\text{O}$  phase. In Figure S1, a representative XRD pattern of the as prepared catalyst is given.

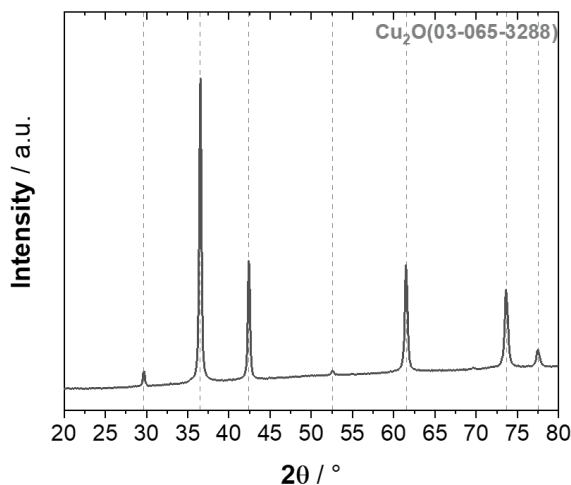


**Figure S1.** XRD pattern of the as prepared  $\text{Cu}_2\text{O}$  particle catalyst with dashed reference lines for indication of the most intense reflections for a  $\text{Cu}_2\text{O}$  (03-065-3288) reference pattern.

The compositional characterization of the cubic Cu<sub>2</sub>O catalyst before and after CO<sub>2</sub>RR has been described in detail in our previous work.<sup>1</sup> Here we observed the reduction of the Cu<sub>2</sub>O phase during application of cathodic potentials towards a predominantly metallic Cu phase with small remnants of an oxidic phase within deeper layers of the material. We like to refer to this work for further information on the compositional changes of the cubic Cu<sub>2</sub>O catalyst during CO<sub>2</sub> electrolysis.

## 2.3 Electrochemical characterization

### *General procedure*

A commercial 4-chamber Micro-Flow-Cell (ElectroCell) was used to perform all electrochemical experiments. Gas diffusion electrodes were prepared by airbrushing a dispersion of the catalyst and Nafion binder (Sigma-Aldrich, 5%) in iso-propanol and ultrapure water (MilliQ) on the microporous side of a carbon gas diffusion layer (Freudenberg H23C2). A commercial IrO<sub>x</sub>-coated Ti sheet (MMO, ElectroCell) was used as anode with an active geometric area of 10 cm<sup>2</sup>. A peristaltic pump (PMP Ecoline, Cole-Parmer) was used to cycle the electrolyte at 100 mL min<sup>-1</sup> through the anode and cathode compartment separated by an anion conducting membrane (Selemion, AMV, AGV Engineering Co., LTD). If not specifically stated otherwise, following parameters were used during the electrochemical characterization:

The gas feed, CO<sub>2</sub> (4.5N), was supplied convectively from the back of the GDL through the catalytic layer of 3 cm<sup>2</sup> active geometric area at a volumetric rate of 50 mL min<sup>-1</sup>, which was regulated using a mass flow controller (Bronkhorst). The same electrolyte (1 M KHCO<sub>3</sub>, each 500 mL, Sigma-Aldrich, BioUltra, ≥99.5%) was used for the anode and cathode compartment and the catholyte was saturated for 30 min with CO<sub>2</sub> prior to reduction experiments. CO<sub>2</sub> reduction electrolysis was conducted galvanostatically with a holding time of two hours at each investigated current step and scanned starting from low towards increasing values. In between different currents potentiostatic impedance spectroscopy at open circuit voltage was used to determine electrolyte resistivity and account for the ohmic drop in calculations of IR-free potentials.

### *Investigation of catalyst loading*

To study the effect of catalyst loading, the volume of ink used during airbrushing was varied, while using a constant ionomer to catalyst ratio of 10wt% (relative to the total combined loading of ionomer and catalyst).

### *Investigation of Nafion content*

In the study of the effect of Nafion content, 6 mg of the catalyst particles with varying amounts of Nafion ionomer were dispersed in a mixture of iso-propanol and water and subsequently airbrushed on the carbon GDL to obtain a relative Nafion content of 0, 5, 10, 30 and 50 wt%. The loading of Cu<sub>2</sub>O particles was kept constant at 0.7 mg cm<sup>-2</sup> throughout the study.

### *Determination of double layer capacitance*

The electrochemical double layer capacitance was determined by cycling the potential between 0.1 V<sub>RHE</sub> and 0.25 V<sub>RHE</sub> under variation of scan rates (20, 50, 80, 100, 150 and 200 mV s<sup>-1</sup>). The capacitance was measured for the studies of Nafion content and catalyst loading, directly after electrolysis in the testing solution of 1 M KHCO<sub>3</sub> electrolyte saturated with CO<sub>2</sub>.

### *Oxygen reduction reaction in the flow-cell*

For experiments involving the oxygen reduction reaction (ORR), a higher concentration of 2 M KHCO<sub>3</sub> was used as electrolyte in order to reduce ohmic losses and maximize ORR currents to help with investigations of the mass transport. At the start of each ORR experiment the cathode potential was cycled in N<sub>2</sub> saturated conditions in between -1.3 and 0.45 V<sub>RHE</sub> at 100 mV s<sup>-1</sup> to electrochemically reduce the catalyst and achieve stable starting conditions. Afterwards, the electrode potential was set to -0.45 V<sub>RHE</sub> and the partial pressure of O<sub>2</sub> in N<sub>2</sub> was gradually increased in the following order: 0.05, 0.1, 0.2, 0.3, 0.5, 0.7 and finally 1.0 bar. Adjustments in O<sub>2</sub> partial pressure were carried out by setting mixtures of N<sub>2</sub> and O<sub>2</sub> gas flowrates, controlled by individual MFCs, while keeping the total volumetric flow at 50 mL min<sup>-1</sup>. Each partial pressure was set for at least 2 min, or until a stable ORR current was observed before moving towards the next, higher value.

### *Investigation of KHCO<sub>3</sub> concentration*

To investigate the effect of KHCO<sub>3</sub> concentration on CO<sub>2</sub>RR selectivity, catalyst inks with various amounts of Nafion were prepared to achieve a constant particle loading of 0.7 mg cm<sup>-2</sup> with three different Nafion contents of 10, 30 and 50 wt% on a total active, geometric area of 1 cm<sup>2</sup>. For each Nafion content, three different catholyte KHCO<sub>3</sub> concentrations (0.1 M, 1.0 M, 3.0 M) were tested, with a constant anolyte concentration of 1.0 M. The convective supply of CO<sub>2</sub> was set to 30 mL min<sup>-1</sup> to account for the reduced geometric area and additional 20 mL min<sup>-1</sup> were introduced

in the electrolyte reservoir to keep the total gas flow directed towards the GC at 50 mL min<sup>-1</sup>. No impedance measurements were performed in between current steps.

## **2.4 Product analysis**

The outgoing CO<sub>2</sub> gas stream with CO<sub>2</sub>RR products from the flow-cell was introduced into a gas chromatograph (GC, Shimadzu GC 2014) equipped with a methanizer and flame ionization detector (FID) for detection of CO, CO<sub>2</sub>, CH<sub>4</sub> and C<sub>2</sub>H<sub>4</sub>, as well as a thermal conductivity detector (TCD) for detection of H<sub>2</sub>.

Liquid products were analyzed with a liquid injection gas chromatograph for detection of alcohols (Shimadzu GC 2010 plus, SH-Stabilwax Capillary Column, FID Detector) and for the detection of carboxylic acids by a high performance liquid chromatograph (HPLC, Agilent 1200 series, Organic-Acid Resin column). For sampling of the liquid products, 2 mL aliquots of the catholyte were taken after constant current steps by an automatic sampling device.

### 3. Physical and chemical characterization

*Additional information on the effect of particle catalyst loading*

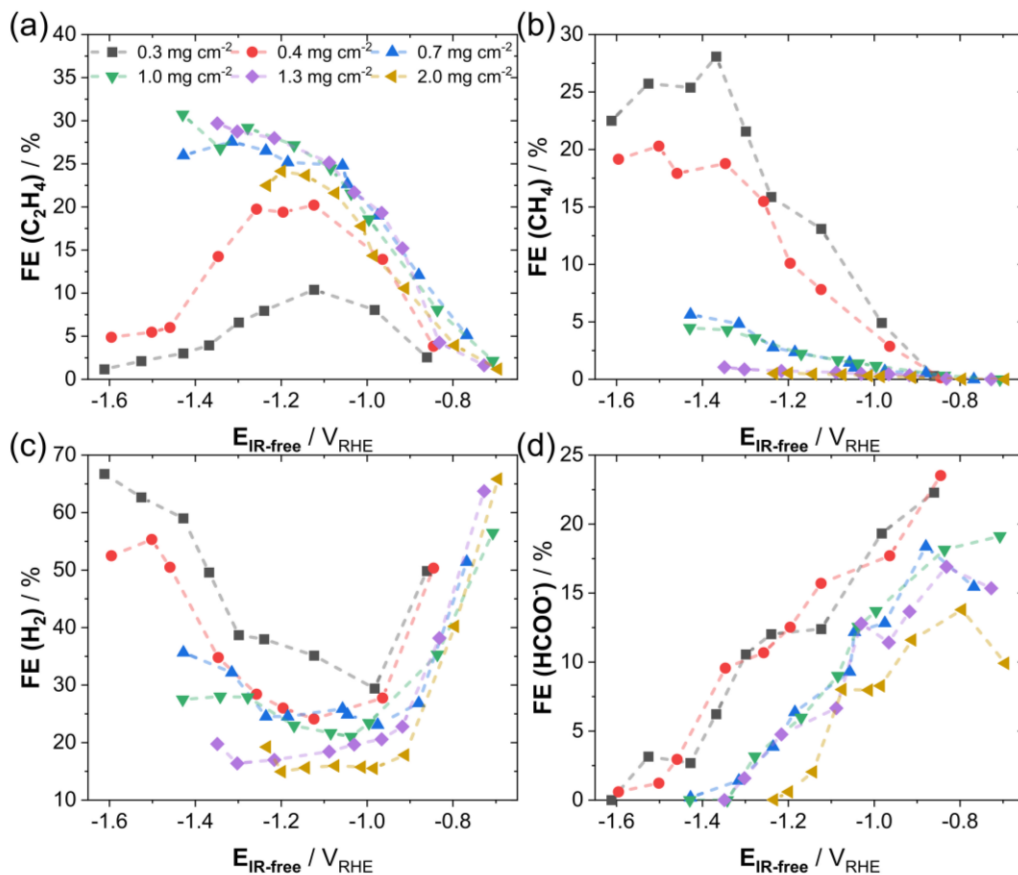


**Figure S2.** Faradaic efficiency as a function of applied IR-free RHE potentials for C<sub>2</sub>H<sub>4</sub> (a), CH<sub>4</sub> (b), H<sub>2</sub> (c) and HCOO<sup>-</sup> (d) during tests in the flow-cell for different catalyst loadings. Test were performed in 1 M KHCO<sub>3</sub> with constant Nafion content of 10 wt% and an active geometric area of 3 cm<sup>2</sup>. Dashed lines are shown to guide the eye.

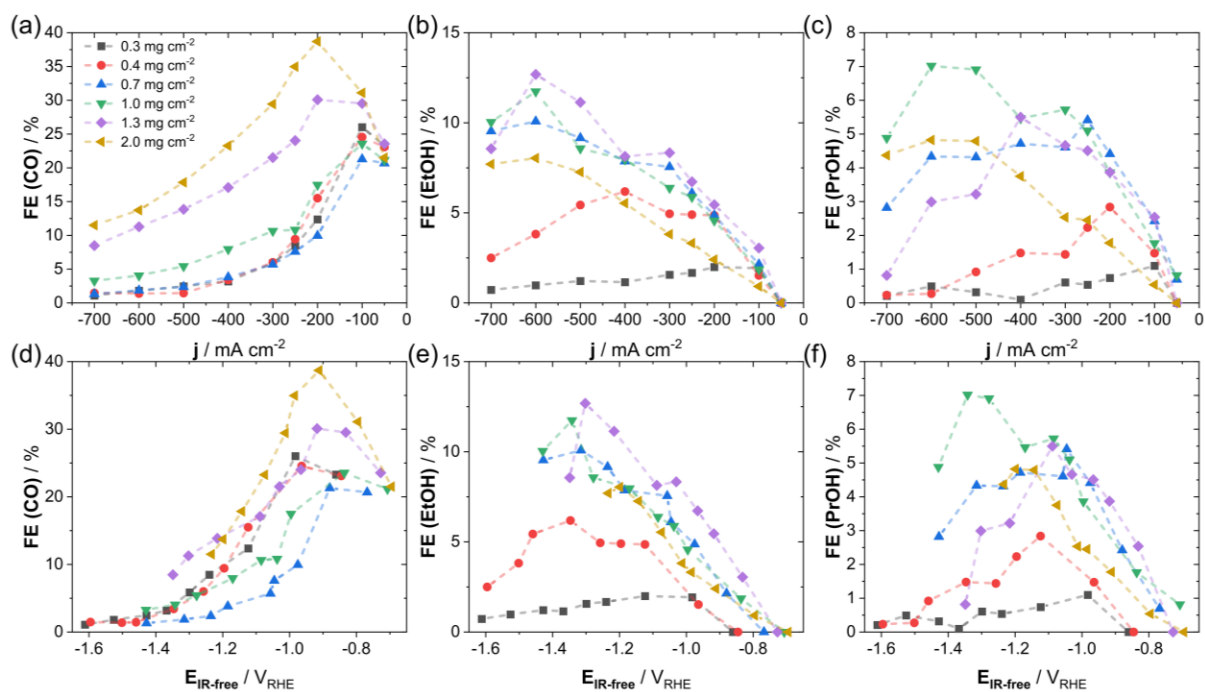


**Figure S3.** Faradaic efficiency as a function of applied current density for CO (a), EtOH (b) and PrOH (c). Faradaic efficiency as a function of applied IR-free RHE potentials for CO (d), EtOH (e) and PrOH (f). Test were performed in 1 M KHCO<sub>3</sub> with constant Nafion content of 10 wt%, various catalyst loadings and an active geometric area of 3 cm<sup>2</sup>. Dashed lines are shown to guide the eye.

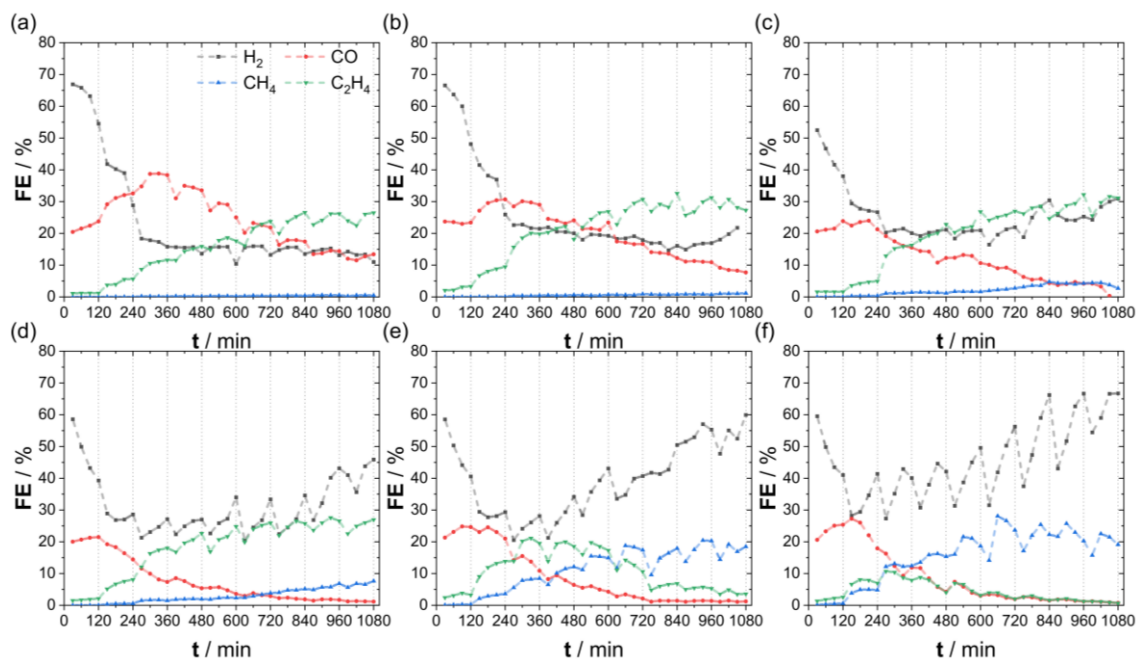


**Figure S4.** Change in faradaic efficiency for gaseous products ( $\text{H}_2$ ,  $\text{CO}$ ,  $\text{CH}_4$  and  $\text{C}_2\text{H}_4$ ) with reaction time for electrodes that show a constant Nafion content of 10 wt% and different particle catalyst loadings:  $2.0 \text{ mg cm}^{-2}$  (a),  $1.3 \text{ mg cm}^{-2}$  (b),  $1.0 \text{ mg cm}^{-2}$  (c),  $0.7 \text{ mg cm}^{-2}$  (d),  $0.4 \text{ mg cm}^{-2}$  (e) and  $0.3 \text{ mg cm}^{-2}$  (f). Horizontal dashed lines indicate a change in applied current density, which was stepwise increased to more cathodic values from  $50 \text{ mA cm}^{-2}$  towards  $700 \text{ mA cm}^{-2}$  with ongoing reaction time.

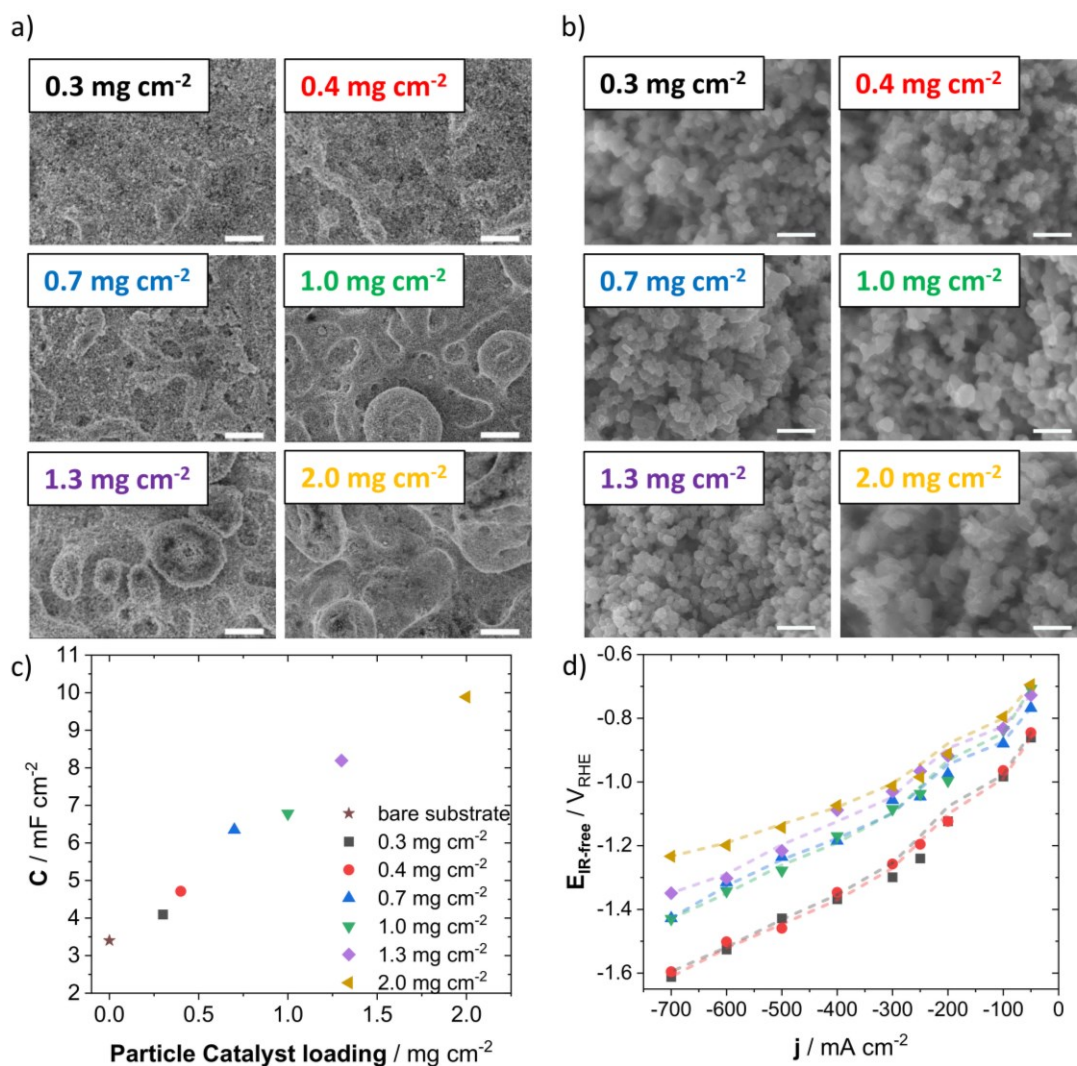


**Figure S5.** Low-magnification (a) and high-magnification (b) top view SEM images after electrolysis, electrochemical double layer capacitance after electrolysis (c) and polarization curves (d) of GDEs with various catalyst mass loadings with dashed lines to guide the eye. Conditions were 3 cm<sup>2</sup> of geometric surface area, 1 M KHCO<sub>3</sub> and 10 wt% of Nafion binder. Scale bars in SEM images represent 400 nm for the case of high-magnification and 10 μm for the case of low-magnification.

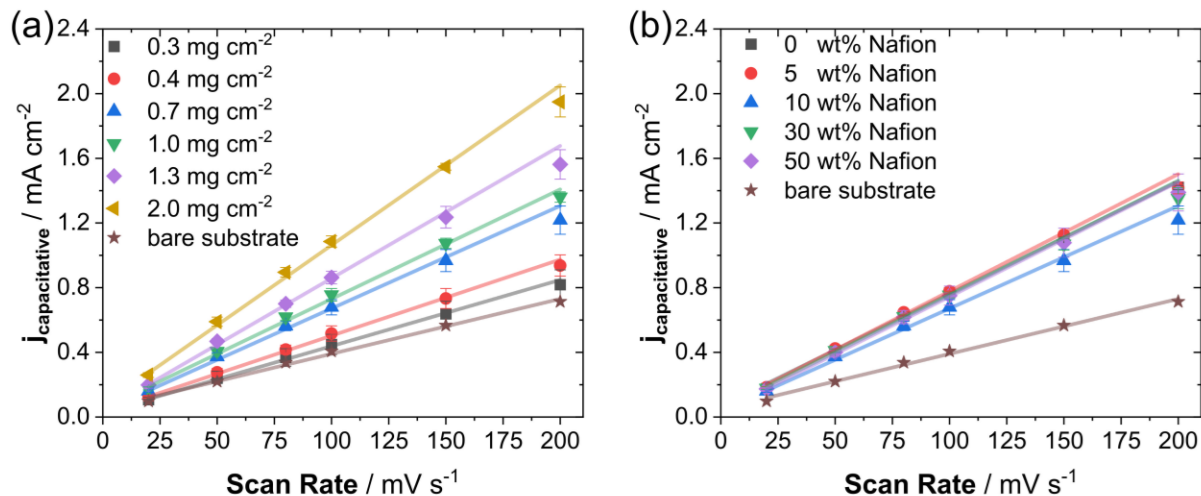


**Figure S6.** Electrochemical capacitance measurements for various particle catalyst loadings (a) and various ionomer contents (b) after  $\text{CO}_2\text{RR}$  electrolysis. The potential was cycled in between  $0.1 V_{\text{RHE}}$  and  $0.25 V_{\text{RHE}}$  at different scan rates directly after screening the catalytic selectivity during  $\text{CO}_2\text{RR}$ . The sample “bare substrate” is referring to an uncoated Freudenberg C2 gas diffusion layer. Tests were performed in 1 M  $\text{KHCO}_3$  with constant Nafion content of 10 wt% (a) or constant particle catalyst loading of  $0.7 \text{ mg cm}^{-2}$  (b) and an active geometric area of  $3 \text{ cm}^2$ .

*Additional information on the effect of ionomer to catalyst ratio*

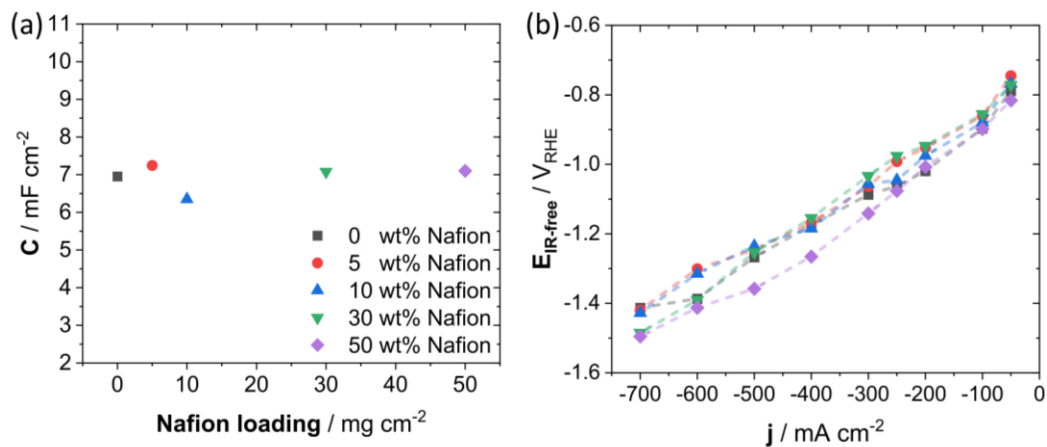


**Figure S7.** Measurements of double layer capacitance (a) and IR-free electrode potentials as function of applied current density with dashed lines to guide the eye (b) for electrodes with various Nafion contents. Conditions were as follows:  $3 \text{ cm}^2$  of geometric surface area,  $1 \text{ M KHCO}_3$  and  $0.7 \text{ mg cm}^{-2}$  catalyst mass loading.

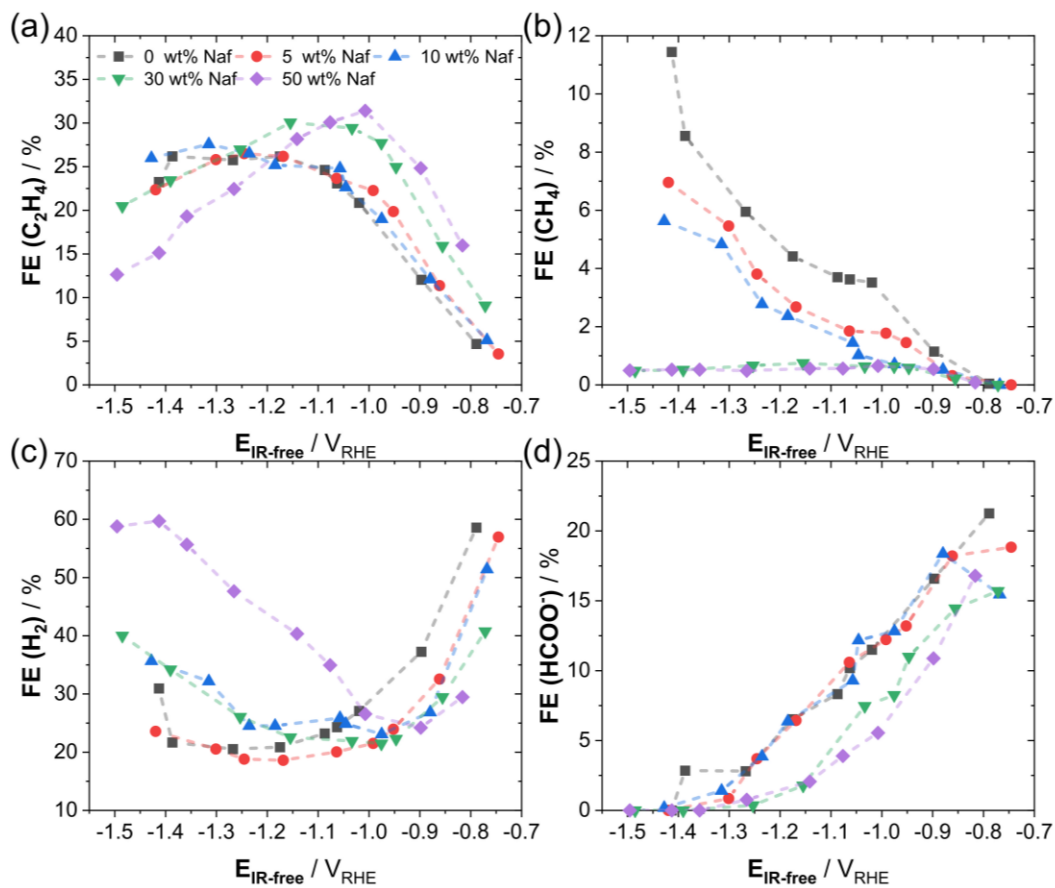


**Figure S8.** Faradaic efficiency as a function of applied IR-free RHE potentials for C<sub>2</sub>H<sub>4</sub> (a), CH<sub>4</sub> (b), H<sub>2</sub> (c) and HCOO<sup>-</sup> (d) during tests in the flow-cell for various different Nafion contents. Tests were performed in 1 M KHCO<sub>3</sub> with constant catalyst loading of 0.7 mg cm<sup>-2</sup> and an active geometric area of 3 cm<sup>2</sup>. Dashed lines are shown to guide the eye.

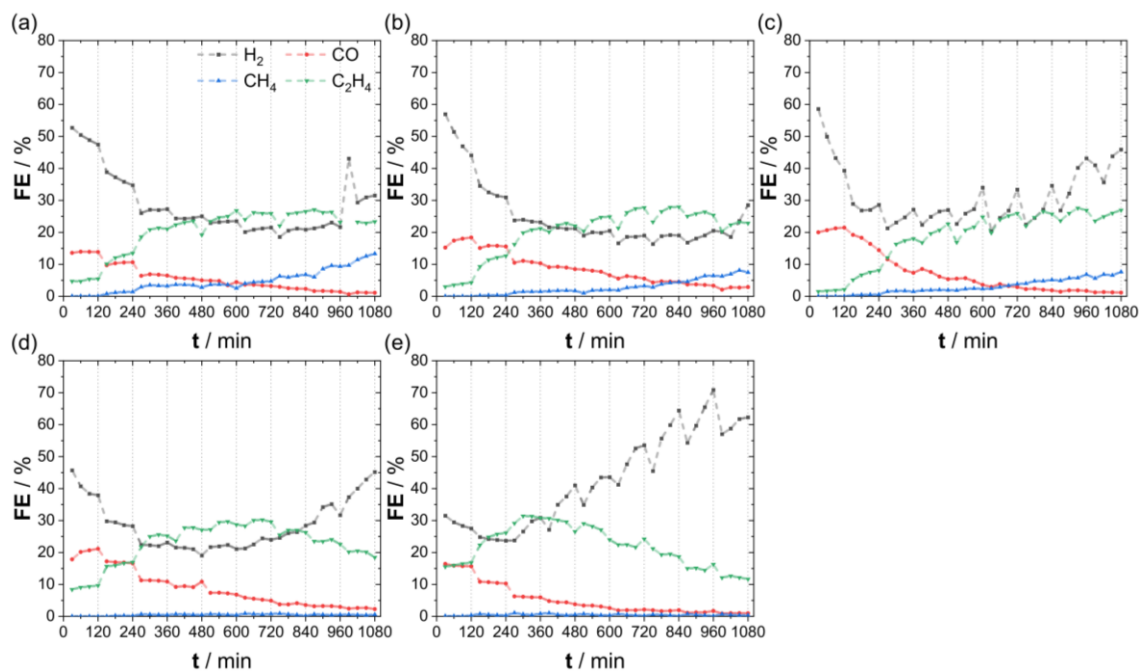


**Figure S9.** Change in faradaic efficiency for gaseous products (H<sub>2</sub>, CO, CH<sub>4</sub> and C<sub>2</sub>H<sub>4</sub>) with reaction time for electrodes that show a constant particle catalyst loading of 0.7 mg cm<sup>-2</sup> and different Nafion contents: 0 wt% (a), 5 wt% (b), 10 wt% (c), 30 wt% (d) and 50 wt% (e). Horizontal dashed lines indicate a change in applied current density, which was stepwise increased to more cathodic values from 50 mA cm<sup>-2</sup> towards 700 mA cm<sup>-2</sup> with ongoing reaction time.

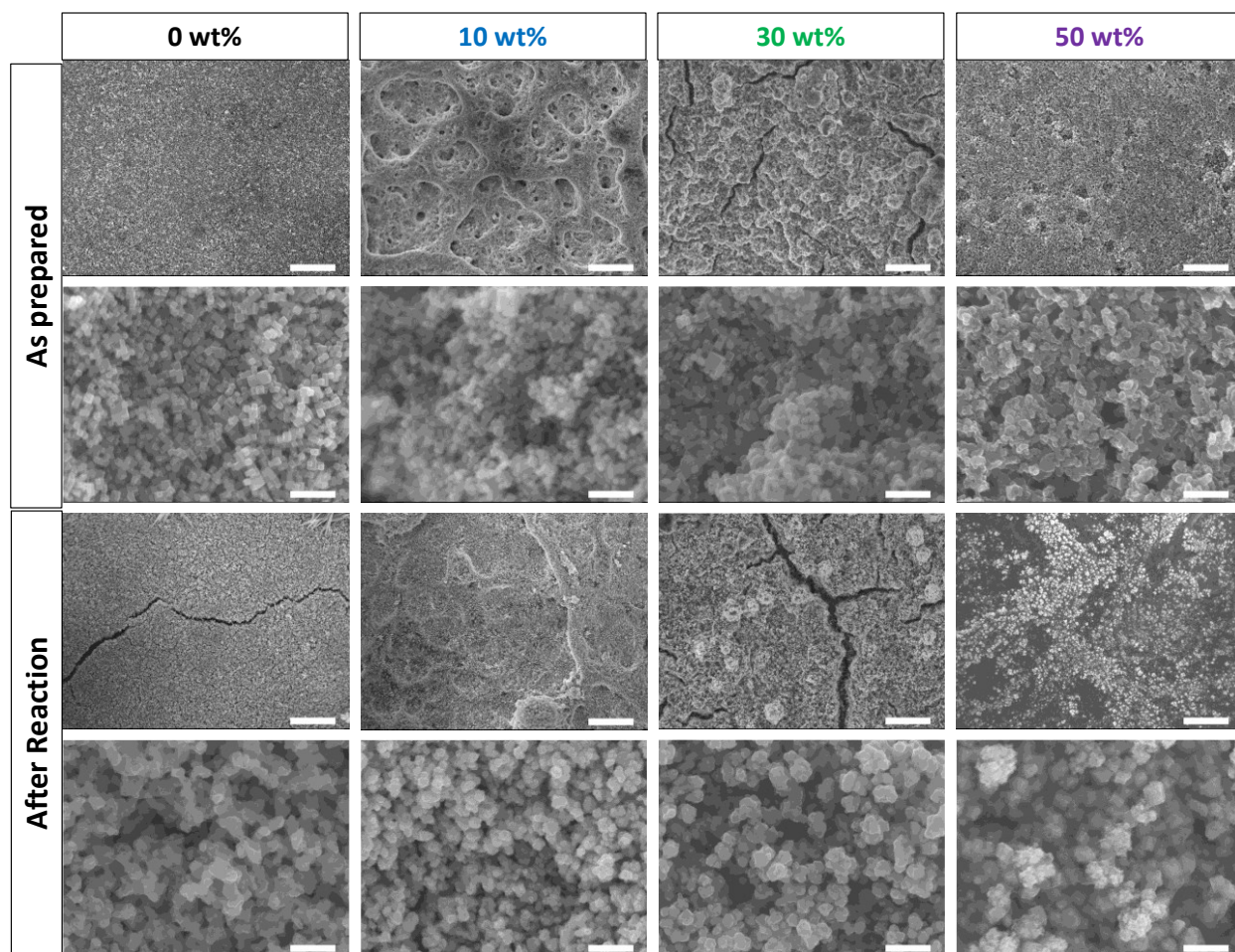


**Figure S10.** Top-view SEM images of GDEs with different Nafion contents, as prepared and after reaction. Tests were performed in 1 M  $\text{KHCO}_3$  with constant catalyst loading of  $0.7 \text{ mg cm}^{-2}$ , various Nafion contents and an active geometric area of  $3 \text{ cm}^2$ . Low magnification images of the first rows for after reaction and as prepared show a scale bar of  $10 \text{ }\mu\text{m}$  and higher magnification images of the second rows show a scale bar of  $400 \text{ nm}$ .

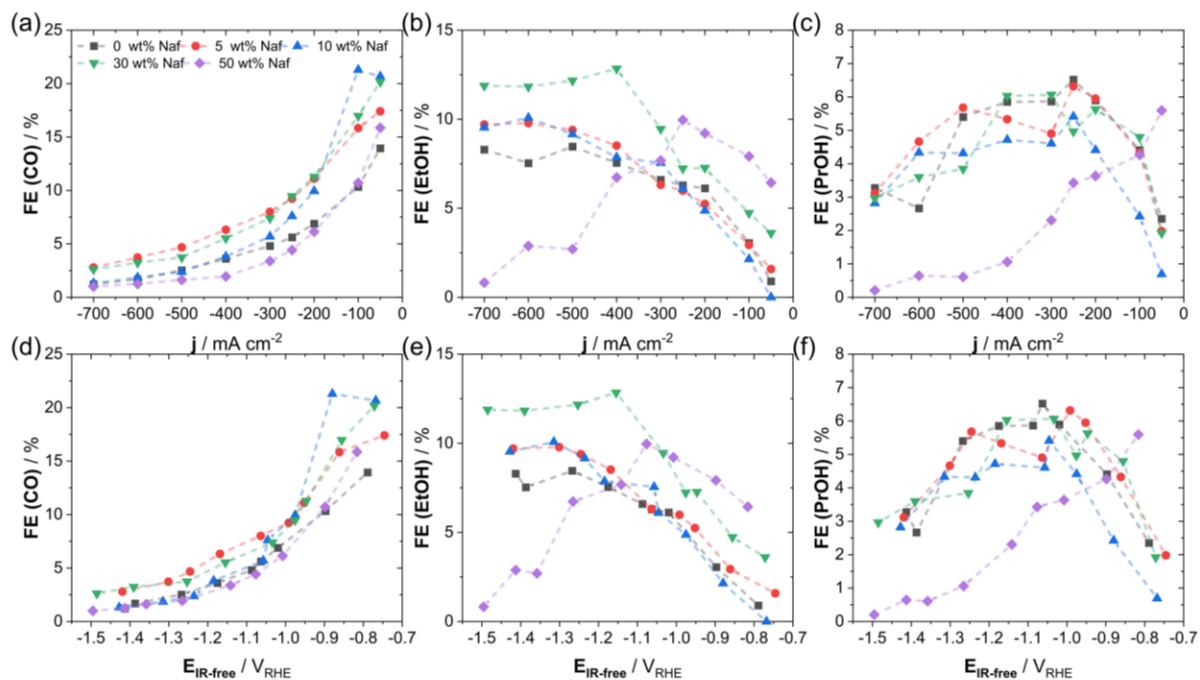


**Figure S11.** Faradaic efficiency as a function of applied current density for CO (a), EtOH (b) and PrOH (c). Faradaic efficiency as a function of applied IR-free RHE potentials for CO (d), EtOH (e) and PrOH (f). Tests were performed in 1 M  $\text{KHCO}_3$  with constant catalyst loading of  $0.7 \text{ mg cm}^{-2}$ , various Nafion contents and an active geometric area of  $3 \text{ cm}^2$ . Dashed lines are shown to guide the eye.

*Additional discussion on the effect of changes in surface morphology of the catalyst layer.*

Generally, one can consider the morphological properties of the electrode on different length scales, ranging from the detailed structure of the individual catalyst particles, over the surface (roughness) of the catalyst layer towards the extended 3-dimensional structure (thickness) of the catalyst layer.

As highly defined, structurally identically Cu<sub>2</sub>O particles were used in the preparation of all electrodes throughout this study, we believe we can exclude major changes in the nanoscopic morphology as origin of the observed differences in CO<sub>2</sub>RR selectivity.

Indeed, variations in ionomer content and particle loading seemed to influence the apparent roughness of the catalytic layer (see Figure S5 and Figure S10). However, we argue that this structural change did not strongly alter the electrochemical properties of the system and is not primarily responsible for the observed selectivity changes.

In case of the ionomer content, the 0 wt% and 50 wt% electrodes were quite comparable in their respective surface structure (see Figure S10), but largely differed in the observed CO<sub>2</sub>RR selectivity (see Figure 3). Furthermore, the relative change in double layer capacitance, as a measure of the ECSA, was minor throughout the investigated ionomer contents (Figure S7). This observation suggests that the roughness of the film was not changed in a significant way by variation of ionomer content.

For the different catalyst particle loadings, the observed increase in double layer capacitance from the lowest loading of 0.3 mg cm<sup>-2</sup> (4 mF cm<sup>-2</sup>) towards the highest loading of 2.0 mg cm<sup>-2</sup> (10 mF cm<sup>-2</sup>) showed a relative increase by a factor of around 2.5 (Figure S5). This corresponds to a rather small increase in ECSA in comparison to other studies discussing roughness effects in H-Cell experiments. Here, an increase in surface areas of 10 to 50-fold in respect to a planer Cu foil are often reported for “high-surface” oxide-derived Cu catalysts. In H-Cell studies, considerable effects of roughness were only achieved, when exceeding a 10-fold increase in roughness referred to a polished Cu foil electrode.<sup>2</sup> In comparison, the changes in surface-roughness discussed throughout our work is rather small and most likely not the exclusive origin of the observed effects.

Furthermore, even if an altered roughness of the catalyst layer is (partly) responsible for the effect discussed within the present study it would still agree with the conclusions drawn in our work. Essentially, an increase in surface roughness can be compared to an increased layer thickness and, therefore, is in line with the suggested concept of altered concentration gradients that cause a variation in catalytic selectivity.



*Additional information on the effect of  $\text{KHCO}_3$  concentration*

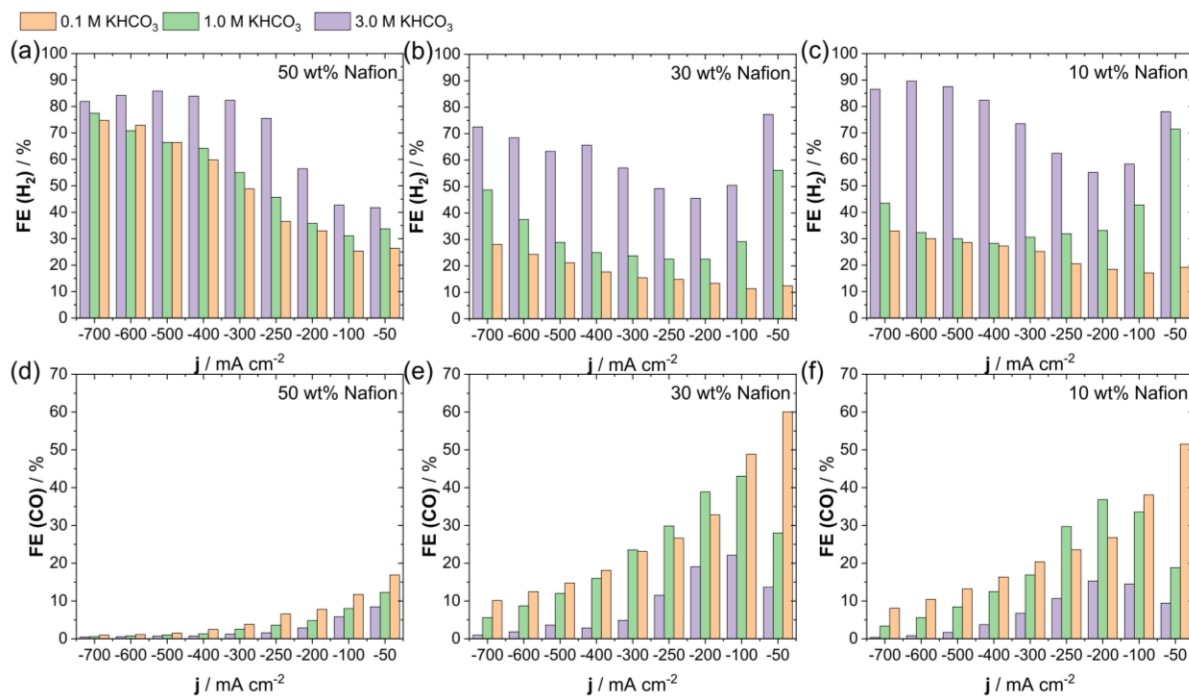


**Figure S12.** Effect of variations in  $\text{KHCO}_3$  concentration on the  $\text{CO}_2\text{RR}$  selectivity towards HER products using 50 wt% (a), 30 wt% (b), and 10 wt% of Nafion (c). Effect of variations in  $\text{KHCO}_3$  concentration on the  $\text{CO}_2\text{RR}$  selectivity towards  $\text{CO}$  using 50 wt% (d), 30 wt% (e), and 10 wt% (f) of Nafion. In all cases,  $\text{Cu}_2\text{O}$  loading was const. at  $0.7 \text{ mg cm}^{-2}$ .

*Additional information on the effect of ionomer to catalyst ratio – ORR*

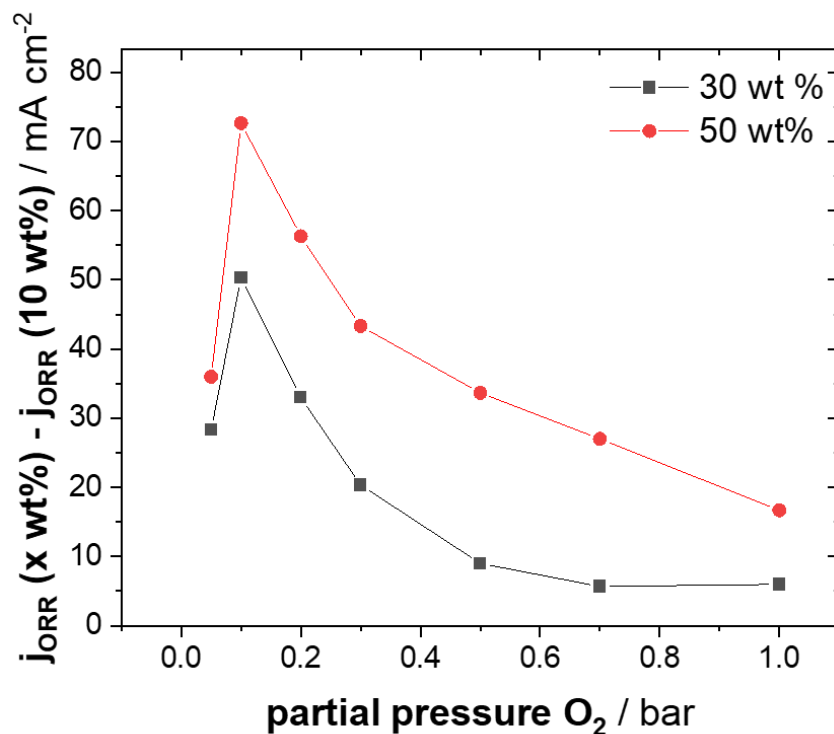


**Figure S13.** Measurements of oxygen reduction reaction (ORR) currents in 2 M  $\text{KHCO}_3$  as a function of partial  $\text{O}_2$  pressure for various Nafion contents. Shown is the difference of the ORR current obtained for the 10 wt% Nafion sample to the ORR current for the 30 wt% sample (black) and the 50 wt% sample (red).

*Supplementary Tables for the effect of particle catalyst loading and ionomer to catalyst ratio*

**Ionomer to catalyst ratio**

	<b>0 wt% Nafion</b>	<b>5 wt% Nafion</b>	<b>10 wt% Nafion</b>	<b>30 wt% Nafion</b>	<b>50 wt% Nafion</b>
<b>Current density</b>	<b>Std. Deviation</b>				
<b>-50</b>	0.053	0.010	0.024	0.008	0.004
<b>-100</b>	0.028	0.023	0.011	0.009	0.006
<b>-200</b>	0.021	0.037	0.062	0.007	0.028
<b>-250</b>	0.004	0.049	0.024	0.008	0.020
<b>-300</b>	0.034	0.020	0.013	0.051	0.032
<b>-400</b>	0.014	0.094	0.061	0.024	0.095
<b>-500</b>	0.012	0.047	0.020	0.111	0.090
<b>-600</b>	0.042	0.020	0.047	0.061	0.041
<b>-700</b>	0.033	0.096	0.051	0.086	0.038

**Table S1.** Polarization curve data for the effect of variations in ionomer (Nafion) to catalyst ratio. The shown standard deviations have been calculated from at least two independent measurements.

	<b>0 wt% Nafion</b>	<b>5 wt% Nafion</b>	<b>10 wt% Nafion</b>	<b>30 wt% Nafion</b>	<b>50 wt% Nafion</b>
<b>Current density</b>	<b>Std. Deviation</b>				
<b>-50</b>	6.1	2.8	2.1	4.6	0.8
<b>-100</b>	1.7	3.2	0.1	5.6	1.2
<b>-200</b>	0.9	2.6	1.6	3.4	5.4
<b>-250</b>	1.4	2.3	2.9	3.5	11.4
<b>-300</b>	1.9	2.3	5.1	6.6	12.8
<b>-400</b>	1.7	1.7	4.8	4.3	11.0
<b>-500</b>	2.3	1.3	5.0	4.1	9.7
<b>-600</b>	7.2	1.1	6.8	6.4	6.0
<b>-700</b>	19.4	6.9	0.4	9.4	2.0

**Table S2.** Faradic efficiency towards H<sub>2</sub> production data for the effect of variations in ionomer (Nafion) to catalyst ratio. The shown standard deviations have been calculated from at least two independent measurements.

	0 wt% Nafion	5 wt% Nafion	10 wt% Nafion	30 wt% Nafion	50 wt% Nafion
<b>Current density</b>	<b>Std. Deviation</b>				
-50	4.01	4.55	3.56	6.13	0.31
-100	1.79	3.44	6.45	5.31	2.22
-200	1.61	2.57	2.43	3.95	1.19
-250	1.23	1.96	1.28	3.70	0.33
-300	0.95	1.95	0.37	3.52	0.24
-400	0.50	1.49	0.03	1.88	0.41
-500	0.35	1.39	0.45	1.18	0.56
-600	0.58	1.28	0.27	1.09	0.58
-700	0.67	1.13	0.21	0.99	0.44

**Table S3.** Faradic efficiency towards CO production data for the effect of variations in ionomer (Nafion) to catalyst ratio. The shown standard deviations have been calculated from at least two independent measurements.

	0 wt% Nafion	5 wt% Nafion	10 wt% Nafion	30 wt% Nafion	50 wt% Nafion
<b>Current density</b>	<b>Std. Deviation</b>				
-50	0.06	0.00	0.00	0.00	0.07
-100	0.56	0.11	0.59	0.25	0.21
-200	0.12	0.59	0.56	0.58	0.13
-250	0.93	0.75	0.88	0.54	0.24
-300	1.12	0.66	1.17	0.52	0.32
-400	2.19	1.19	1.58	0.55	0.29
-500	2.58	0.57	1.03	0.44	0.37
-600	1.76	1.96	3.08	0.36	0.27
-700	0.18	2.42	3.88	0.37	0.32

**Table S4.** Faradic efficiency towards CH<sub>4</sub> production data for the effect of variations in ionomer (Nafion) to catalyst ratio. The shown standard deviations have been calculated from at least two independent measurements.

	<b>0 wt% Nafion</b>	<b>5 wt% Nafion</b>	<b>10 wt% Nafion</b>	<b>30 wt% Nafion</b>	<b>50 wt% Nafion</b>
<b>Current density</b>	<b>Std. Deviation</b>				
<b>-50</b>	6.64	1.64	1.59	3.93	1.19
<b>-100</b>	6.35	1.91	3.93	3.72	2.16
<b>-200</b>	4.00	1.86	1.94	2.81	1.60
<b>-250</b>	2.83	0.97	0.24	2.98	0.35
<b>-300</b>	2.87	1.19	1.88	2.45	0.36
<b>-400</b>	3.26	1.25	1.86	1.28	1.89
<b>-500</b>	1.76	2.53	3.46	1.85	2.08
<b>-600</b>	4.48	3.83	1.68	3.05	3.12
<b>-700</b>	1.52	4.07	3.10	3.19	2.52

**Table S5.** Faradic efficiency towards C<sub>2</sub>H<sub>4</sub> production data for the effect of variations in ionomer (Nafion) to catalyst ratio. The shown standard deviations have been calculated from at least two independent measurements.

	<b>0 wt% Nafion</b>	<b>5 wt% Nafion</b>	<b>10 wt% Nafion</b>	<b>30 wt% Nafion</b>	<b>50 wt% Nafion</b>
<b>Current density</b>	<b>Std. Deviation</b>				
<b>-50</b>	0.61	0.53	0.00	1.87	2.01
<b>-100</b>	2.01	0.97	0.60	1.75	2.36
<b>-200</b>	0.82	1.37	1.24	0.14	0.61
<b>-250</b>	1.15	1.07	2.10	1.83	3.04
<b>-300</b>	1.22	0.86	2.25	0.48	1.80
<b>-400</b>	1.52	0.34	0.48	1.15	2.23
<b>-500</b>	0.28	0.92	1.96	1.98	0.76
<b>-600</b>	0.44	1.38	2.89	0.56	1.75
<b>-700</b>	4.63	1.84	0.52	2.42	1.16

**Table S6.** Faradic efficiency towards EtOH production data for the effect of variations in ionomer (Nafion) to catalyst ratio. The shown standard deviations have been calculated from at least two independent measurements.

	<b>0 wt% Nafion</b>	<b>5 wt% Nafion</b>	<b>10 wt% Nafion</b>	<b>30 wt% Nafion</b>	<b>50 wt% Nafion</b>
<b>Current density</b>	<b>Std. Deviation</b>				
<b>-50</b>	1.81	0.32	0.98	1.11	2.33
<b>-100</b>	2.32	0.80	1.61	0.15	1.59
<b>-200</b>	1.18	0.56	2.15	0.22	0.40
<b>-250</b>	0.33	0.41	2.53	0.56	0.81
<b>-300</b>	1.03	1.31	1.43	0.42	0.03
<b>-400</b>	1.36	1.58	1.48	0.92	0.93
<b>-500</b>	1.00	1.47	1.00	0.38	0.58
<b>-600</b>	0.94	0.56	2.19	0.02	0.91
<b>-700</b>	2.81	1.46	0.01	0.42	0.29

**Table S7.** Faradic efficiency towards PrOH production data for the effect of variations in ionomer (Nafion) to catalyst ratio. The shown standard deviations have been calculated from at least two independent measurements.

	<b>0 wt% Nafion</b>	<b>5 wt% Nafion</b>	<b>10 wt% Nafion</b>	<b>30 wt% Nafion</b>	<b>50 wt% Nafion</b>
<b>Current density</b>	<b>Std. Deviation</b>				
<b>-50</b>	2.15	1.74	2.68	1.09	2.14
<b>-100</b>	2.72	1.50	1.73	1.60	3.24
<b>-200</b>	0.85	0.61	0.17	2.40	4.43
<b>-250</b>	2.06	0.31	1.78	3.05	3.39
<b>-300</b>	2.37	5.98	0.28	2.13	2.63
<b>-400</b>	2.47	0.42	2.26	1.04	0.97
<b>-500</b>	0.11	0.60	0.06	0.63	0.00
<b>-600</b>	0.17	1.20	0.06	0.00	0.00
<b>-700</b>	0.00	0.00	0.26	0.00	0.00

**Table S8.** Faradic efficiency towards HCOO<sup>-</sup> production data for the effect of variations in ionomer (Nafion) to catalyst ratio. The shown standard deviations have been calculated from at least two independent measurements.

## Particle catalyst loading

	0.3 mg cm <sup>-2</sup>	0.4 mg cm <sup>-2</sup>	0.7 mg cm <sup>-2</sup>	1.0 mg cm <sup>-2</sup>	1.3 mg cm <sup>-2</sup>	2.0 mg cm <sup>-2</sup>
Current density	Std. Deviation					
-50	0.03	0.00	0.02	0.01	0.06	0.00
-100	0.02	0.02	0.01	0.02	0.03	0.02
-200	0.05	0.05	0.06	0.01	0.05	0.03
-250	0.02	0.05	0.02	0.04	0.05	0.02
-300	0.00	0.05	0.01	0.06	0.10	0.04
-400	0.08	0.10	0.06	0.04	0.07	0.01
-500	0.05	0.07	0.02	0.04	0.06	0.02
-600	0.01	0.12	0.05	0.01	0.02	0.03
-700	0.03	0.09	0.05	0.05	0.05	0.04

**Table S9.** Polarization curve data for the effect of variations in particle catalyst loading. The shown standard deviations have been calculated from at least two independent measurements.

	0.3 mg cm <sup>-2</sup>	0.4 mg cm <sup>-2</sup>	0.7 mg cm <sup>-2</sup>	1.0 mg cm <sup>-2</sup>	1.3 mg cm <sup>-2</sup>	2.0 mg cm <sup>-2</sup>
Current density	Std. Deviation					
-50	5.51	0.29	2.13	9.11	5.70	8.98
-100	3.39	1.17	0.11	1.04	9.13	1.27
-200	0.85	0.15	1.61	3.94	0.80	5.71
-250	0.24	1.26	2.86	2.88	1.59	6.04
-300	2.19	6.83	5.05	0.68	1.90	5.92
-400	4.60	9.69	4.82	3.15	2.91	6.21
-500	16.60	7.74	4.96	9.97	3.24	4.79
-600	8.05	7.26	6.76	13.30	1.84	3.84
-700	5.06	6.36	0.37	9.20	4.84	3.33

**Table S10.** Faradic efficiency towards H<sub>2</sub> production data for the effect of variations in particle catalyst loading. The shown standard deviations have been calculated from at least two independent measurements.

	<b>0.3 mg cm<sup>-2</sup></b>	<b>0.4 mg cm<sup>-2</sup></b>	<b>0.7 mg cm<sup>-2</sup></b>	<b>1.0 mg cm<sup>-2</sup></b>	<b>1.3 mg cm<sup>-2</sup></b>	<b>2.0 mg cm<sup>-2</sup></b>
<b>Current density</b>	<b>Std. Deviation</b>					
<b>-50</b>	0.14	1.26	3.56	0.52	0.82	1.89
<b>-100</b>	4.49	0.58	6.45	7.51	0.37	4.53
<b>-200</b>	0.99	1.74	2.43	9.00	1.58	9.01
<b>-250</b>	0.05	0.73	1.28	3.36	0.07	8.73
<b>-300</b>	0.13	0.80	0.37	6.48	0.86	7.26
<b>-400</b>	0.92	1.44	0.03	4.41	1.13	5.36
<b>-500</b>	0.34	1.37	0.45	3.14	0.21	3.02
<b>-600</b>	0.21	0.49	0.27	2.60	0.03	2.36
<b>-700</b>	0.11	0.32	0.21	3.95	0.08	3.05

**Table S11.** Faradic efficiency towards CO production data for the effect of variations in particle catalyst loading. The shown standard deviations have been calculated from at least two independent measurements.

	<b>0.3 mg cm<sup>-2</sup></b>	<b>0.4 mg cm<sup>-2</sup></b>	<b>0.7 mg cm<sup>-2</sup></b>	<b>1.0 mg cm<sup>-2</sup></b>	<b>1.3 mg cm<sup>-2</sup></b>	<b>2.0 mg cm<sup>-2</sup></b>
<b>Current density</b>	<b>Std. Deviation</b>					
<b>-50</b>	0.32	0.05	0.00	0.00	0.00	0.00
<b>-100</b>	1.62	0.01	0.59	0.31	0.01	0.02
<b>-200</b>	2.21	0.92	0.56	0.71	0.12	0.03
<b>-250</b>	3.40	1.35	0.88	0.72	0.13	0.05
<b>-300</b>	1.86	5.28	1.17	0.67	0.03	0.00
<b>-400</b>	0.50	3.15	1.58	0.46	0.07	0.04
<b>-500</b>	5.41	1.58	1.03	1.22	0.12	0.02
<b>-600</b>	0.51	2.55	3.08	1.29	0.13	0.15
<b>-700</b>	4.16	1.99	3.88	2.96	0.06	0.30

**Table S12.** Faradic efficiency towards CH<sub>4</sub> production data for the effect of variations in particle catalyst loading. The shown standard deviations have been calculated from at least two independent measurements.

	<b>0.3 mg cm<sup>-2</sup></b>	<b>0.4 mg cm<sup>-2</sup></b>	<b>0.7 mg cm<sup>-2</sup></b>	<b>1.0 mg cm<sup>-2</sup></b>	<b>1.3 mg cm<sup>-2</sup></b>	<b>2.0 mg cm<sup>-2</sup></b>
<b>Current density</b>	<b>Std. Deviation</b>					
<b>-50</b>	1.00	1.31	1.59	3.04	0.43	1.41
<b>-100</b>	1.39	3.18	3.93	4.37	0.66	4.24
<b>-200</b>	1.00	7.12	1.94	4.36	0.87	5.62
<b>-250</b>	0.72	4.58	0.24	2.26	0.61	6.05
<b>-300</b>	0.66	7.78	1.88	0.89	0.56	4.15
<b>-400</b>	0.13	1.75	1.86	4.35	0.67	3.05
<b>-500</b>	0.41	4.02	3.46	6.64	1.01	1.19
<b>-600</b>	0.12	0.21	1.68	4.47	1.06	0.55
<b>-700</b>	0.17	0.81	3.10	7.06	3.10	1.31

**Table S13.** Faradic efficiency towards C<sub>2</sub>H<sub>4</sub> production data for the effect of variations in particle catalyst loading. The shown standard deviations have been calculated from at least two independent measurements.

	<b>0.3 mg cm<sup>-2</sup></b>	<b>0.4 mg cm<sup>-2</sup></b>	<b>0.7 mg cm<sup>-2</sup></b>	<b>1.0 mg cm<sup>-2</sup></b>	<b>1.3 mg cm<sup>-2</sup></b>	<b>2.0 mg cm<sup>-2</sup></b>
<b>Current density</b>	<b>Std. Deviation</b>					
<b>-50</b>	0.00	0.00	0.00	0.00	0.00	0.00
<b>-100</b>	0.26	1.89	0.60	0.83	2.09	0.78
<b>-200</b>	0.64	0.66	1.24	0.01	2.41	0.48
<b>-250</b>	0.75	0.27	2.10	0.58	1.61	0.27
<b>-300</b>	0.24	0.38	2.25	0.06	1.68	0.26
<b>-400</b>	0.25	1.44	0.48	0.70	2.74	0.24
<b>-500</b>	0.44	2.11	1.96	1.88	0.83	0.79
<b>-600</b>	0.43	1.68	2.89	2.41	0.80	0.84
<b>-700</b>	0.16	2.75	0.52	1.40	1.90	0.04

**Table S14.** Faradic efficiency towards EtOH production data for the effect of variations in particle catalyst loading. The shown standard deviations have been calculated from at least two independent measurements.

	<b>0.3 mg cm<sup>-2</sup></b>	<b>0.4 mg cm<sup>-2</sup></b>	<b>0.7 mg cm<sup>-2</sup></b>	<b>1.0 mg cm<sup>-2</sup></b>	<b>1.3 mg cm<sup>-2</sup></b>	<b>2.0 mg cm<sup>-2</sup></b>
<b>Current density</b>	<b>Std. Deviation</b>					
<b>-50</b>	0.00	0.00	0.98	1.15	0.00	0.00
<b>-100</b>	0.23	1.88	1.61	0.71	2.90	0.49
<b>-200</b>	0.33	0.06	2.15	0.80	2.67	0.50
<b>-250</b>	0.29	0.49	2.53	0.01	3.14	0.14
<b>-300</b>	0.75	0.80	1.43	0.64	2.64	0.99
<b>-400</b>	0.13	0.73	1.48	1.47	0.67	0.76
<b>-500</b>	0.45	0.60	1.00	0.76	1.45	0.84
<b>-600</b>	0.05	0.09	2.19	0.40	1.08	1.92
<b>-700</b>	0.10	0.33	0.01	2.35	1.15	1.57

**Table S15.** Faradic efficiency towards PrOH production data for the effect of variations in particle catalyst loading. The shown standard deviations have been calculated from at least two independent measurements.

	<b>0.3 mg cm<sup>-2</sup></b>	<b>0.4 mg cm<sup>-2</sup></b>	<b>0.7 mg cm<sup>-2</sup></b>	<b>1.0 mg cm<sup>-2</sup></b>	<b>1.3 mg cm<sup>-2</sup></b>	<b>2.0 mg cm<sup>-2</sup></b>
<b>Current density</b>	<b>Std. Deviation</b>					
<b>-50</b>	0.70	2.14	2.68	1.32	3.19	4.37
<b>-100</b>	1.15	0.55	1.73	1.41	3.34	0.12
<b>-200</b>	2.11	3.34	0.17	0.10	1.26	0.94
<b>-250</b>	4.66	3.61	1.78	0.78	1.45	1.72
<b>-300</b>	0.78	1.87	0.28	3.73	2.87	1.60
<b>-400</b>	2.06	3.06	2.26	0.23	0.10	0.71
<b>-500</b>	0.06	2.11	0.06	0.16	0.90	0.19
<b>-600</b>	0.60	1.10	0.06	0.00	0.16	0.84
<b>-700</b>	0.00	0.04	0.26	0.00	0.00	0.03

**Table S16.** Faradic efficiency towards HCOO<sup>-</sup> production data for the effect of variations in particle catalyst loading. The shown standard deviations have been calculated from at least two independent measurements.

## Effect of KHCO<sub>3</sub> concentration

	0.1 M KHCO <sub>3</sub>		1.0 M KHCO <sub>3</sub>		3.0 M KHCO <sub>3</sub>	
	C <sub>2+</sub> C <sub>2</sub> H <sub>4</sub> , EtOH, PrOH	C <sub>1</sub> CH <sub>4</sub> , HCOO <sup>-</sup>	C <sub>2+</sub> C <sub>2</sub> H <sub>4</sub> , EtOH, PrOH	C <sub>1</sub> CH <sub>4</sub> , HCOO <sup>-</sup>	C <sub>2+</sub> C <sub>2</sub> H <sub>4</sub> , EtOH, PrOH	C <sub>1</sub> CH <sub>4</sub> , HCOO <sup>-</sup>
Current density [mA cm <sup>-2</sup> ]	Std. Deviation	Std. Deviation	Std. Deviation	Std. Deviation	Std. Deviation	Std. Deviation
-50	7.63	2.02	0.49	0.00	0.00	1.32
-100	12.20	1.80	2.01	1.78	0.00	1.85
-200	10.08	0.81	6.10	2.41	1.71	3.48
-250	12.78	1.47	5.51	0.47	1.63	1.62
-300	12.86	0.87	3.50	0.72	1.63	1.97
-400	9.84	0.63	7.36	1.34	1.62	1.50
-500	8.61	0.72	9.27	1.37	0.38	1.19
-600	7.02	0.65	7.01	2.34	0.20	1.95
-700	4.80	0.84	4.65	2.09	0.21	0.83
	H <sub>2</sub>	CO	H <sub>2</sub>	CO	H <sub>2</sub>	CO
Current density [mA cm <sup>-2</sup> ]	Std. Deviation	Std. Deviation	Std. Deviation	Std. Deviation	Std. Deviation	Std. Deviation
-50	0.66	13.89	2.42	3.91	5.62	0.51
-100	4.91	12.76	2.20	4.19	4.41	0.55
-200	2.66	14.32	0.67	3.90	7.36	0.58
-250	4.27	13.44	0.46	3.82	8.10	1.81
-300	2.71	11.93	5.29	13.17	6.75	1.47
-400	3.23	9.54	7.34	9.66	3.45	0.75
-500	3.06	7.85	7.28	6.56	0.08	0.02
-600	2.59	6.33	9.18	4.60	3.71	0.03
-700	1.88	4.52	10.99	2.17	5.15	0.09

**Table S17.** Faradic efficiency towards C<sub>2+</sub>, C<sub>1</sub>, H<sub>2</sub> and CO production data for the effect of variations KHCO<sub>3</sub> electrolyte concentration for electrodes prepared with 10 wt% Nafion. The shown standard deviations have been calculated from at least two independent measurements.

	0.1 M KHCO <sub>3</sub>		1.0 M KHCO <sub>3</sub>		3.0 M KHCO <sub>3</sub>	
	C <sub>2+</sub> C <sub>2</sub> H <sub>4</sub> , EtOH, PrOH	C <sub>1</sub> CH <sub>4</sub> , HCOO <sup>-</sup>	C <sub>2+</sub> C <sub>2</sub> H <sub>4</sub> , EtOH, PrOH	C <sub>1</sub> CH <sub>4</sub> , HCOO <sup>-</sup>	C <sub>2+</sub> C <sub>2</sub> H <sub>4</sub> , EtOH, PrOH	C <sub>1</sub> CH <sub>4</sub> , HCOO <sup>-</sup>
Current density [mA cm <sup>-2</sup> ]	Std. Deviation	Std. Deviation	Std. Deviation	Std. Deviation	Std. Deviation	Std. Deviation
-50	6.05	2.68	6.40	0.75	0.00	0.74
-100	4.59	2.93	7.02	0.98	5.29	3.47
-200	3.54	1.97	6.38	1.63	3.13	0.53
-250	5.10	1.13	5.81	1.75	3.37	0.98
-300	5.61	0.49	10.25	2.13	6.52	2.14
-400	7.47	0.37	6.38	0.39	2.33	0.30
-500	6.05	0.10	5.44	0.94	9.91	0.84
-600	5.16	0.04	8.17	0.35	5.84	1.05
-700	5.88	0.11	3.73	0.35	3.93	0.09
	H <sub>2</sub>	CO	H <sub>2</sub>	CO	H <sub>2</sub>	CO
Current density [mA cm <sup>-2</sup> ]	Std. Deviation	Std. Deviation	Std. Deviation	Std. Deviation	Std. Deviation	Std. Deviation
-50	3.11	15.90	2.03	1.80	1.94	0.63
-100	3.33	13.09	7.12	3.63	0.64	0.04
-200	4.73	10.03	2.42	0.76	1.00	2.14
-250	4.62	8.37	4.33	1.26	3.09	3.50
-300	4.68	8.06	5.87	2.44	3.26	1.19
-400	3.86	7.83	4.21	0.78	4.83	0.42
-500	5.97	7.70	3.52	0.10	6.94	2.99
-600	8.53	7.18	4.08	0.66	1.75	1.14
-700	11.64	8.79	10.47	1.12	3.34	0.34

**Table S18.** Faradic efficiency towards C<sub>2+</sub>, C<sub>1</sub>, H<sub>2</sub> and CO production data for the effect of variations KHCO<sub>3</sub> electrolyte concentration for electrodes prepared with 30 wt% Nafion. The shown standard deviations have been calculated from at least two independent measurements.

	0.1 M KHCO <sub>3</sub>		1.0 M KHCO <sub>3</sub>		3.0 M KHCO <sub>3</sub>	
	C <sub>2+</sub> C <sub>2</sub> H <sub>4</sub> , EtOH, PrOH	C <sub>1</sub> CH <sub>4</sub> , HCOO <sup>-</sup>	C <sub>2+</sub> C <sub>2</sub> H <sub>4</sub> , EtOH, PrOH	C <sub>1</sub> CH <sub>4</sub> , HCOO <sup>-</sup>	C <sub>2+</sub> C <sub>2</sub> H <sub>4</sub> , EtOH, PrOH	C <sub>1</sub> CH <sub>4</sub> , HCOO <sup>-</sup>
Current density [mA cm <sup>-2</sup> ]	Std. Deviation	Std. Deviation	Std. Deviation	Std. Deviation	Std. Deviation	Std. Deviation
-50	6.38	6.96	8.78	1.58	8.60	4.57
-100	2.44	5.66	7.08	2.49	5.78	0.32
-200	8.41	2.58	3.58	2.64	4.06	2.37
-250	7.34	2.41	7.25	1.42	6.89	1.06
-300	3.26	1.69	8.32	1.06	4.74	1.83
-400	1.15	0.61	7.60	0.66	4.33	0.25
-500	9.51	0.07	6.70	0.25	2.59	0.05
-600	9.13	0.07	6.96	0.26	1.95	0.04
-700	12.04	0.35	6.73	0.30	1.85	0.02
	H <sub>2</sub>	CO	H <sub>2</sub>	CO	H <sub>2</sub>	CO
Current density [mA cm <sup>-2</sup> ]	Std. Deviation	Std. Deviation	Std. Deviation	Std. Deviation	Std. Deviation	Std. Deviation
-50	3.36	2.24	6.09	5.05	5.88	0.64
-100	2.85	4.09	9.82	3.80	9.12	0.17
-200	5.68	3.72	13.01	1.89	11.30	0.28
-250	10.43	3.94	15.19	1.14	9.29	0.36
-300	8.94	2.02	6.60	1.17	5.28	0.31
-400	15.33	0.07	9.24	0.84	4.42	0.38
-500	9.15	0.62	1.04	0.80	2.92	0.15
-600	3.82	0.80	1.68	0.64	2.01	0.01
-700	2.49	0.43	12.27	0.58	0.89	0.05

**Table S19.** Faradic efficiency towards C<sub>2+</sub>, C<sub>1</sub>, H<sub>2</sub> and CO production data for the effect of variations KHCO<sub>3</sub> electrolyte concentration for electrodes prepared with 50 wt% Nafion. The shown standard deviations have been calculated from at least two independent measurements.

## References

1. T. Möller, F. Scholten, T. N. Thanh, I. Sinev, J. Timoshenko, X. Wang, Z. Jovanov, M. Glied, B. Roldan Cuenya, A. S. Varela and P. Strasser, *Angew. Chem. Int. Ed.*, 2020, **59**, 17974-17983.
2. Y. Lum, B. Yue, P. Lobaccaro, A. T. Bell and J. W. Ager, *J. Phys. Chem. C*, 2017, **121**, 14191-14203.